Elasticity of Cobalt at High Pressure Studied by Inelastic X-Ray Scattering

F Antonangeli, F M Krisch, F M Fiquet, F L Farber, C M Aracne, F M Badro, F L Occelli, H Requardt

HAL Id: insu-01387217

https://insu.hal.science/insu-01387217

Submitted on 25 Oct 2016

Elasticity of Cobalt at High Pressure Studied by Inelastic X-Ray Scattering

D. Antonangeli,[1] M. Krisch,[1] G. Fiquet,[2] D. L. Farber,[3] C. M. Aracne,[3] J. Badro,[2,3] F. Occelli,[3] and H. Requardt[1]

[1]*European Synchrotron Radiation Facility, B.P. 220, F-38043 Grenoble Cedex, France*
[2]*Laboratoire de Minéralogie et Cristallographie, UMR CNRS 7590, Institut de Physique du Globe de Paris, Université Paris VI,*
4 Place Jussieu, 75252 Paris Cedex 05, France
[3]*Earth Science Division, Energy and Environment Directorate, Lawrence Livermore National Laboratory,*
7000 East Avenue, Livermore, California 94550, USA

The five independent elastic moduli of single-crystalline hcp cobalt were determined by inelastic x-ray scattering to 39 GPa and compared to ultrasonic measurements and first principles calculations. In general the agreement is good, in particular, for the evolution of the longitudinal sound velocity in the *a-c* plane. This confirms the calculations, suggesting that a similar evolution is valid for hcp iron, the main constituent of the Earth's inner core, up to the highest investigated pressure. Our results represent an important benchmark to further refine *ab initio* calculations.

Characterizing the effect of pressure on the propagation of elastic waves in condensed matter is singularly important for understanding elasticity, mechanical stability of solids, material strength, interatomic interactions, and phase transition mechanisms. The high pressure elastic properties of hexagonal-closed-packed (hcp) metals have attracted a great deal of recent interest, not only for their intriguing properties such as, for example, the eventual existence of an electronic topological transition in zinc [1] and osmium [2] and of magnetoelastic effects in cobalt [3], but also since they represent a challenge for the most advanced *ab initio* calculations [4]. A further important case is related to the elasticity of hcp iron, the main constituent of the Earth's core [5,6]. While nowadays it is well established, mainly by seismic travel time analysis and free oscillation studies, that Earth's inner core is elastically anisotropic [7,8], the origin of this anisotropy is still poorly understood. Theoretical attempts to calculate the elastic moduli of iron yield very different results that are in disagreement with the scarce experimental results [9,10]. Possible causes for this are the following: (i) the difficulty to perform reliable calculations at high pressures and temperatures and (ii) the impossibility to carry out experiments on single crystal hcp iron, because of the bcc-to-hcp transition at about 13 GPa, which does not allow the preservation of the single-crystalline state.

In this Letter, we present the first experimental determination of the five independent elastic moduli of hcp cobalt under hydrostatic compression to 39 GPa. Cobalt is a $3d$ transition metal and is located next to iron in the periodic table. The mechanical and thermal properties of these two elements are close, and, most importantly, *ab initio* calculations [4] show that hcp Fe and hcp Co display a very similar pressure evolution of the elastic moduli at 0 K. Furthermore, the hcp phase of cobalt is stable at ambient temperature to 100 GPa [11]. Thus, the knowl-

edge of the elasticity of cobalt can be utilized to address the issue of the elastic anisotropy of hcp iron.

Experiments at high pressure are extremely challenging, and thus there are continuous efforts both to improve the traditional methods as well as to develop new techniques, aimed at the experimental determination of elastic properties. However, all the techniques currently employed have limitations in either the highest attainable pressure, the nature of the materials that can be studied, or the information content [12]. Inelastic x-ray scattering (IXS) instead is particularly well suited for studying elastic properties at high pressure. Thanks to the high brilliance of third generation synchrotron sources and efficient x-ray focusing optics, samples with a volume as small as 10^{-5} mm^3 can be probed. This in turn permits the use of diamond anvil cells (DAC), and thus the access to the megabar range. The sound velocities V are directly determined from the linear part of the acoustic phonon branches, and are related to the elastic moduli via the Christoffel equation [13].

Our experiments were carried out on the IXS beam line II (ID28) at the European Synchrotron Radiation Facility in Grenoble, France. The instrument was operated using the Si (9 9 9) configuration, with an incident photon energy of 17.794 keV and a total instrumental energy resolution of 3 meV full-width-half-maximum (FWHM). The dimensions of the focused x-ray beam were 25×60 μm^2 (horizontal $\times$ vertical, FWHM), further reduced by slits for the smallest samples. The momentum resolution was set to 0.3 nm^{-1}. Further experimental details can be found elsewhere [14].

High quality single crystals (45 to 85 μm diameter, 20 μm thickness) were prepared at the Lawrence Livermore National Laboratory, using femtosecond laser cutting and state-of-the-art polishing techniques [15]. The samples were loaded in DACs, using helium as pressure transmitting medium [16] in order to ensure

hydrostatic pressure conditions. For one run neon was used rather than helium, recording values for the elastic moduli in excellent agreement with the ones previously obtained (see Fig. 2), clearly demonstrating that gas absorption by the sample, as well as other pressure medium effects are negligible. Typical mosaic spreads (rocking curves) amounted to 0.1° to 0.2°, and no degradation was observed even for the highest pressure point. Pressure was determined by ruby fluorescence and cross checked with the known cobalt equation of state [11,17]. All crystals were cut with the surface normal parallel to the [110] direction. By simple rotation of the cell around the incident beam direction, this allows access to the longitudinal acoustic (LA) phonon branches along the [100] and [001] direction, the two transverse acoustic (TA) branches along the [110] direction, and the quasi-longitudinal branch along the [101] direction. For the first four directions, the sound velocity is directly related to a specific elastic modulus [for example, $V_{LA[100]} = (C_{11}/\rho)^{1/2}$], namely C_{11} (LA[100]), C_{33} (LA[001]), C_{66} [18] ($TA[110]_{\langle 100 \rangle}$), and C_{44} ($TA[110]_{\langle 001 \rangle}$), while the longitudinal sound velocity along the [101] direction is a function of all five elastic moduli, so that the knowledge of the first four allows determining C_{13} [13]. In Fig. 1 we report examples of the collected IXS spectra. These are characterized by an elastic contribution centered at zero energy and two symmetric features, the Stokes and anti-Stokes peaks of the cobalt acoustic phonons. The energy position $E(q)$ of the phonons was extracted using a model function composed of a sum of Lorentzian functions, for which the inelastic contributions were constrained by the Bose factor at 300 K. This model function was convoluted with the experimentally determined resolution function and fitted to the IXS spectra, utilizing a standard χ^2 minimization routine. Typically, two to five IXS spectra were recorded in the low q part of the acoustic phonon branch, and the sound velocity was determined by a linear fit to the $E(q)$ values with an error of 1%–2%. In parallel to the IXS spectra, the Bragg angles of the [100], [002], and [101] reflections were recorded, in order to provide an independent determination of the density for each pressure point, obtaining values in agreement with the equation of state of polycrystalline cobalt in helium [19]. This allowed us to derive the elastic moduli with an indetermination of 2% to 4% for C_{11}, C_{33}, C_{44}, and C_{66}, while, due to the error propagation, the error amounts to 4% to 7% for C_{12} and to about 15% for C_{13}. The pressure evolution of the elastic moduli is reported in Fig. 2. The pressure derivatives of the various C_{ij} are well described by a linear law (see solid lines in Fig. 2). We note that $C_{11}(P = 0) < C_{33}(P = 0)$ and $(\partial C_{11}/\partial P) < (\partial C_{33}/\partial P)$, so that the elastic anisotropy between the basal (a-b) plane and the c axis, already present at ambient condition, is increasing with pressure. Furthermore, $C_{44}(P = 0) > C_{66}(P = 0)$, while for other hcp metals such as beryllium, rhenium, zinc, and zirconium [20], $C_{66}(P = 0) >$
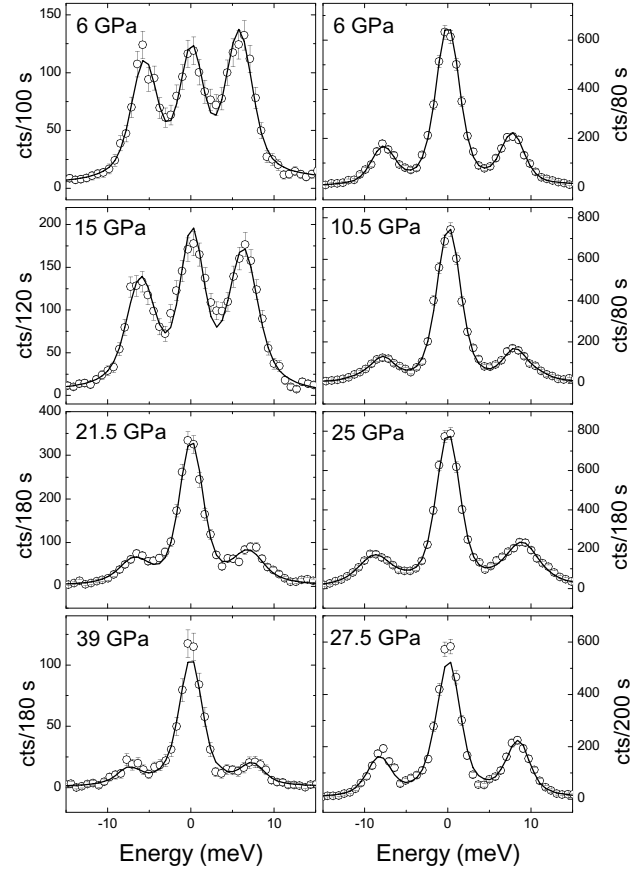

FIG. 1.   Representative IXS spectra of single crystal hcp Co at fixed exchange momentum transfer and different pressures. Left column: $LA[100]$ phonon for $Q(1.05; 0; 0)$; right column $TA[110]_{\langle 001 \rangle}$ phonon for $Q(0.075; -0.15; 2)$. The experimental spectra (open circles) are shown together with their best fits. The relative intensities of the phonons with respect to the elastic line is linked to the intrinsic quality of the samples and resulted to be independent from the pressure.

$C_{44}(P = 0)$. This anomaly disappears with increasing pressure, since $(\partial C_{44}/\partial P) < (\partial C_{66}/\partial P)$, leading to a crossing of the two moduli at about 12 ± 4 GPa. Our results are in good agreement with ambient pressure ultrasonic measurements [20], except for C_{12}, where the IXS value is lower by about 11%. Results from *ab initio* calculations [4,21] yield in most of the cases higher values, with the exception of C_{13}. The calculated pressure evolution is close to the experimentally determined one for C_{11}, C_{33}, C_{66}, and C_{12}, but $\partial C_{44}/\partial P$ and $\partial C_{13}/\partial P$ are, respectively, too high and too low. The IXS results, as well as the ultrasonic measurements and the calculations are summarized in Table I. A more critical comparison suggests that the calculations tend to underestimate the increasing anisotropy between C_{33} and C_{11}, and, above all, do not predict the observed crossing between C_{44} and C_{66}, because of the high value for the C_{44} pressure derivative. In general we observe a better quantitative agreement (in particular for C_{11} and C_{66}) with calculations performed within the local density approximation (LDA)
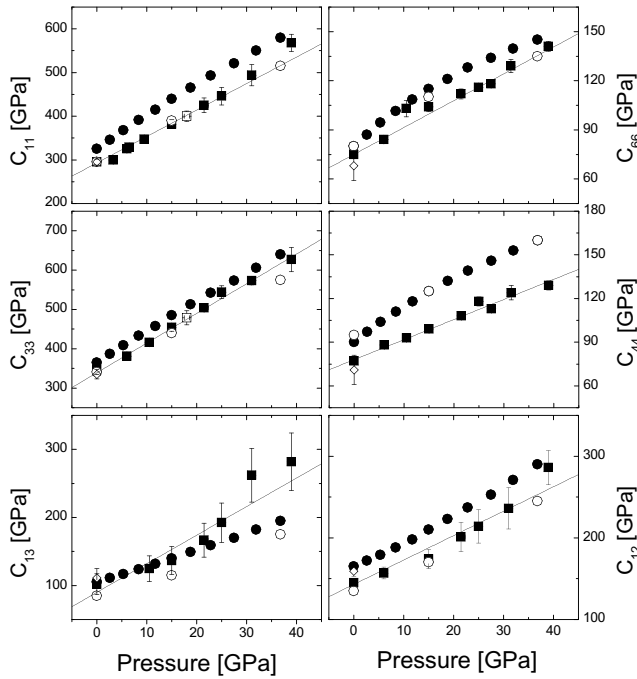
FIG. 2. Pressure evolution of the hcp Co elastic moduli. IXS results, obtained using helium (full squares) and neon (open squares) as pressure transmitting medium; ambient pressure ultrasonic measurements (open diamonds) [20]; *ab initio* calculations within the GGA approximation (full circles) and LDA approximation (open circles) [4,21]. The pressure values for the calculations were obtained using our measured equation of state. The solid line is a linear fit to our data.

rather than within the generalized gradient approximation (GGA), while the IXS values for C_{33} and C_{12} lie in between the two approximations.

The determination of the full elastic tensor and its pressure evolution allows to derive the complete velocity profile of the hcp cobalt crystal. Of particular interest is the sound velocity in the meridian (*a-c*) plane, where all three modes (one longitudinal and two nondegenerate transverse) show an evident directional dependence, as illustrated in Fig. 3. Of these, the variation of the longitudinal sound velocity $V_L(\xi)$ is of central interest since, in the case of iron, it is directly correlated with the observed seismic-wave anisotropy in Earth's inner core [8]. The

upper panel of Fig. 3 shows $V_L(\xi)$ as a function of the propagation direction in the meridian plane, from the *c* to the *a* axis, measured by IXS on cobalt, calculated in GGA and LDA approximation for cobalt [4], and calculated in GGA approximation for iron [4,22]. The results are compared at the same compression ratio $\rho_0/\rho = 0.87$, corresponding to pressures of about 36 GPa for cobalt and about 39 GPa for iron. Although the comparison can only be qualitative, we observe a substantial agreement concerning the shape of $V_L(\xi)$ between our measurements and the calculations in the case of cobalt while, as we already stressed, the magnitude of the calculated anisotropy is underestimated by about a factor of 2. This comparison suggests a sigmoidal shape of $V_L(\xi)$ for hcp iron as well, as indeed the calculations show. This is in contrast with the proposed shape obtained from x-ray radial diffraction measurements, performed on nonhydrostatically compressed polycrystalline hcp iron at 39 GPa [10]. There, the sound dispersion yields almost equal values parallel to the *c* and *a* axes, with a maximum of about 8% higher at 45°.

Concerning the transverse modes, reported in the bottom panel of Fig. 3, we note a good agreement between the experimentally determined and calculated $V_{T1}(\xi)$: the calculations straddle the cobalt IXS measurements. $V_{T1}(\xi)$ for iron displays the same shape, but with a weaker variation of the sound speed, like for $V_L(\xi)$. For $V_{T2}(\xi)$ the disagreement in the case of cobalt is instead evident. Calculations predict a sigmoidal shape with a higher sound velocity along the *c* axis, while the IXS results show a sigmoidal shape with a higher sound velocity along the *a* axis. This is a direct consequence of the already discussed high-pressure crossing between C_{44} and C_{66}, observed in the cobalt experiment, but not predicted by the calculations. The experimental determined shape of $V_{T2}(\xi)$ compares instead well with the theoretical curve for hcp Fe.

In summary, we observe a "regular" behavior of the elastic moduli of hcp cobalt up to 39 GPa. While there are discrepancies between our IXS results and calculation, there is a good overall agreement. The present experimental results are therefore of great value for further refinement of the *ab initio* methods, and might be used to

TABLE I. Zero pressure elastic moduli (in GPa) and their pressure derivatives, obtained by linear fit to the IXS results, and to the calculated values in GGA and LDA approximations. The reported indeterminations are the statistical errors to the fits. The ultrasonic values at ambient condition are the ones reported in [20].

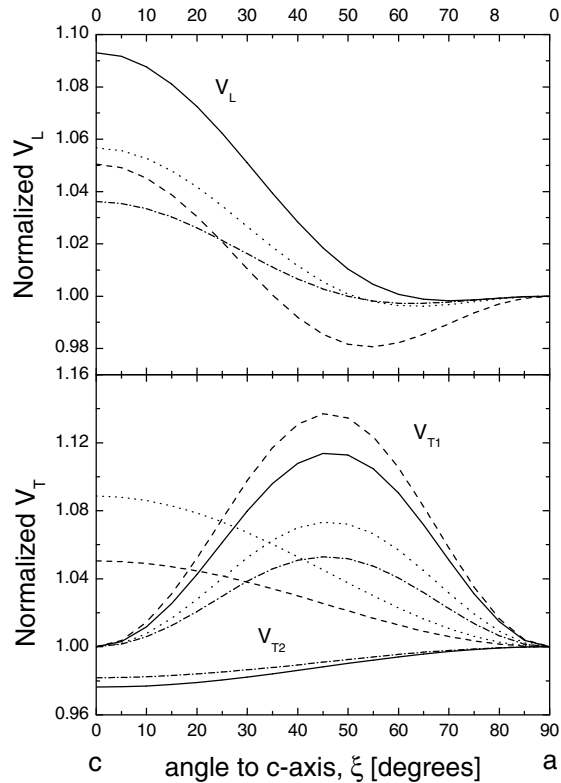|	IXS $C_{ij}(P=0)$	IXS $\partial C_{ij}/\partial P$	US $C_{ij}(P=0)$	GGA $C_{ij}(P=0)$	GGA $\partial C_{ij}/\partial P$	LDA $C_{ij}(P=0)$	LDA $\partial C_{ij}/\partial P$
C_{11}	293 ± 2	6.1 ± 0.4	295 ± 7	331 ± 2	6.9 ± 0.1	297 ± 4	6.0 ± 0.2
C_{33}	339 ± 4	7.6 ± 0.2	335 ± 12	369 ± 2	7.45 ± 0.08	342 ± 3	6.4 ± 0.1
C_{66}	75 ± 2	1.64 ± 0.07	68 ± 9	85 ± 2	1.75 ± 0.09	83 ± 5	1.5 ± 0.2
C_{44}	78 ± 1	1.38 ± 0.05	71 ± 10	94 ± 1	1.89 ± 0.06	96 ± 2	1.7 ± 0.2
C_{13}	90 ± 10	4.2 ± 0.6	111 ± 14	104.0 ± 0.4	2.43 ± 0.02	82 ± 5	2.5 ± 0.2
C_{12}	143 ± 4	3.0 ± 0.4	159 ± 6	161 ± 1	3.40 ± 0.07	131 ± 7	3.0 ± 0.3

FIG. 3. Normalized acoustic sound velocities as a function of the propagation direction in the meridian plane, from the c to the a axis. Upper panel: longitudinal acoustic sound velocity. Lower panel: transverse acoustic sound velocities. Solid line: IXS measurements on hcp Co; dashed line: GGA calculations for hcp Co [4,21]; dotted line: LDA calculations for hcp Co [4]; dash-dotted line: GGA calculations for hcp Fe [4,22].

directly address the choice of the pseudopotential, the treatment of electron correlation and exchange interactions, as well as the applied strains used for the determination of the elastic moduli. We note that the substantial agreement between our experimental results and calculations [4] for the shape of the V_L anisotropy further validates the theoretical results. Last, we suggest that the analogy in terms of elastic properties between hcp Co and hcp Fe, which has been inferred by *ab initio* calculations [4], is valid at least up to 39 GPa. These calculations, together with our new experimental results, provide strong evidence for the sigmoidal shape of the longitudinal sound anisotropy in hcp iron at high pressure and ambient temperature.

Finally, our results on the high pressure elastic properties of hcp cobalt illustrate the power of IXS as a tool to study elasticity under extreme conditions. Indeed, IXS affords the determination of elastic moduli with an accuracy of a few percent. Furthermore, the technique can be applied to a large variety of samples (opaque or transparent, insulating or metallic), probing ordered (single crystals and powders) as well as disordered (liquids and glasses) states.

[1] S. Klotz, M. Braden, and J. M. Besson, Phys. Rev. Lett. **81**, 1239 (1998).

[2] F. Occelli, D. L. Farber, J. Badro, C. M. Aracne, D. M. Teter, M. Hanfland, B. Canny, and B. Couzinet, Phys. Rev. Lett. **93**, 09552 (2004).

[3] A. F. Goncharov, J. Crowhurst, and J. M. Zaug, Phys. Rev. Lett. **92**, 115502 (2004).

[4] G. Steinle-Neumann, L. Stixrude, and R. E. Cohen, Phys. Rev. B **60**, 791 (1999).

[5] F. Birch, J. Geophys. Res. **57**, 227 (1952).

[6] A. Jephcoat and P. Olson, Nature (London) **325**, 332 (1987).

[7] J. H. Woodhouse, D. Giardini, and X. D. Li, Geophys. Res. Lett. **13**, 1549 (1986).

[8] K. G. Creager, Nature (London) **356**, 309 (1992).

[9] D. Antonangeli, F. Occelli, H. Requardt, J. Badro, G. Fiquet, and M. Krisch, Earth Planet. Sci. Lett. **225**, 243 (2004).

[10] H. K. Mao, J. Shu, G. Shen, R. J. Hemley, B. Li, and A. K. Singh, Nature (London) **396**, 741 (1998); Nature (London) **399(E)**, 280 (1999).

[11] C. S. Yoo, H. Cynn, P. Söderlind, and V. Iota, Phys. Rev. Lett. **84**, 4132 (2000).

[12] G. Fiquet, J. Badro, F. Guyot, Ch. Bellin, M. Krisch, D. Antonangeli, H. Requardt, A. Mermet, D. Farber, C. Aracne-Ruddle, and J. Zhang, Phys. Earth Planet. Inter. **143–144**, 5 (2004).

[13] B. A. Auld, *Acoustic Fields and Waves in Solids* (J. Wiley and Sons, New York, 1973), Vol. 1.

[14] M. Krisch, J. Raman Spectrosc. **34**, 628 (2003).

[15] C. Aracne *et al.*, EoS Trans. AGU, 84 (46), Fall Meeting Supplement, Abstract V42A-0333, 2003.

[16] B. Couzinet, N. Dahan, G. Hamel, and J. C. Chervin, High Press. Res. **23**, 409 (2003).

[17] H. Fujihisa and K. Takemura, Phys. Rev. B **54**, 5 (1996).

[18] In the following, we will consider $C_{66} = \frac{1}{2}(C_{11} - C_{12})$ rather then C_{12}, since C_{66} is (as C_{44}) directly linked to a transverse acoustic phonon branch. The derived values for C_{12} are reported for completeness as well.

[19] D. Antonangeli *et al.* (to be published).

[20] H. R. Schober and H. Dederichs, in *Elastic Piezoelectric Pyroelectric Piezooptic Electrooptic Constants and Nonlinear Dielectric Susceptibilities of Crystals*, Landolt-Börnstedt New Series III Vol. 11a (Springer, Berlin, 1979).

[21] G. Steinle-Neumann (private communication).

[22] L. Stixrude and R. E. Cohen, Science **267**, 1972 (1995).